Proceedings of the European Conference Physics of Magnetism 2011 (PM'11), Poznań, June 27–July 1, 2011

Influence of Transition and Rare Earth Elements on Magnetic Properties of Fe–Nb–B–M (M = Ni, Ag, Gd, Tb) Bulk Nanocrystalline Alloys

G. Ziółkowski[a,*], N. Randrianantoandro[b], A. Chrobak[a], J. Klimontko[a], M. Kądziołka-Gaweł[a] and G. Haneczok[c]

[a]Institute of Physics, Silesian University, Uniwersytecka 4, 40-007 Katowice, Poland

[b]Laboratoire de Physique de l'Etat Condensé, UMR CNRS 6087, Université du Maine 72085 Le Mans cedex 9, France

[c]Institute of Materials Science, University of Silesia, Bankowa 12, 40-007 Katowice, Poland

In this work we present magnetic properties of the $(Fe_{80}Nb_6B_{14})_{1-x}M_x$ (where M = Ni, Ag, Gd, Tb and x = 0.08, 0.16, 0.32) bulk nanocrystalline alloys prepared by making use of mould casting technique. The applied preparation technique is favorable to nanocrystallization of the alloys with mean diameters of crystallites ranged from about 10 nm to 30 nm. Phase identification reveals a formation of ternary $RE_2Fe_{14}B$ and binary $REFe_2$ phases dependently on the alloy composition. It was found that for the alloys with Ag addition magnetic moment of Fe atom increases from 2.26 μ_B to 3.36 μ_B for x = 0.08 and x = 0.32, respectively. For Ni addition this quantity decreases with increasing x due to appearing of Fe–Ni (fcc) phases. For Gd, Tb additions the alloys are ferrimagnetic with compensation composition ranged between x = 0.08 and x = 0.16. The both rare earth alloying additions cause a significant magnetic hardening especially in the case of Tb.

PACS: 81.07.Bc, 75.50.Tt, 75.60.−d, 76.80.+y

1. Introduction

Fe-based nanocrystalline materials exhibit, in a comparison with their crystalline form, unique physical properties. Such materials can be fabricated by crystallization of an amorphous precursor which can lead to formation of a certain kind of nanostructure [1, 2]. In this field very interesting are nanocrystalline alloys in the so-called bulk form i.e. rods, ingots etc. with dimensions in order of several mm [3–7]. Among a number of Fe-based nanocrystalline alloys a special meaning have the so-called Nanoperm alloys type i.e. alloy containing Fe as a main element and other additions like Nb and B. For example, a proper thermal annealing of $Fe_{80}Nb_6B_{14}$ amorphous melt spun ribbon leads firstly to a structural relaxation and secondly to nano and full crystallization which cause significant changes of its physical properties [8–10].

The main goal of the work is to study an influence of the alloying additions of transition (M = Ni, Ag) and rare earth (M = Gd, Tb) elements on magnetic and structural properties of the $(Fe_{80}Nb_6B_{14})_{1-x}M_x$ (x = 0.08, 0.16, 0.32) bulk nanocrystalline alloys prepared by the use of mould casting technique.

* corresponding author; e-mail: gzzk@wp.pl

2. Experimental procedure

The samples $(Fe_{80}Nb_6B_{14})_{1-x}$ M_x (M = Ni, Ag, Gd, Tb and x = 0.08, 0.16, 0.32) were prepared by means of the mould casting technique (described in [11]). The applied mould allows obtaining bulk rods of 1.5 mm in diameter and about 3 cm in length. Magnetic measurements were carried out by applying of: (i) the SQUID magnetometer in the temperature range 2–300 K and magnetic field up to 7 T and (ii) magnetic balance in the temperature range 300–1100 K. Phase identification was performed with the use of X-ray diffraction (XRD) in a θ–2θ diffractometer (Siemens D-500) using Cu K_α radiation (1.5418 Å) and ^{57}Fe Mössbauer spectrometry in transmission geometry with constant acceleration spectrometer, using a ^{57}Co source diffused in a rhodium matrix. The ^{57}Fe Mössbauer spectra were recorded at room temperature.

3. Results and discussion

Figure 1 shows an example of XRD patterns for the $(Fe_{80}Nb_6B_{14})_{1-x}Tb_x$ (x = 0.08, 0.16, 0.32) alloys. From such pictures the phases formed during fabrication were detected and additionally a mean crystallite size (from a broadening of the main peak) was calculated. In the as-quenched state all the studied alloys were nanocrystalline and the mean diameter of crystallites are ranged from 12 nm to 28 nm. In order to make the phase detection more precise the Mössbauer measurements were carried out. An example of the Mössbauer spectrum for

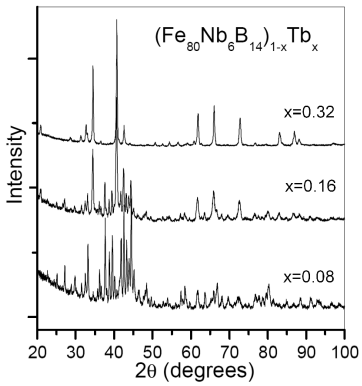

Fig. 1. XRD patterns for the $(Fe_{80}Nb_6B_{14})_{1-x}Tb_x$ alloys.

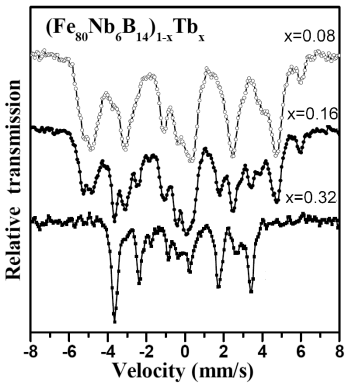

Fig. 2. Mössbauer spectrum for the $(Fe_{80}Nb_6B_{14})_{1-x}Tb_x$ alloys.

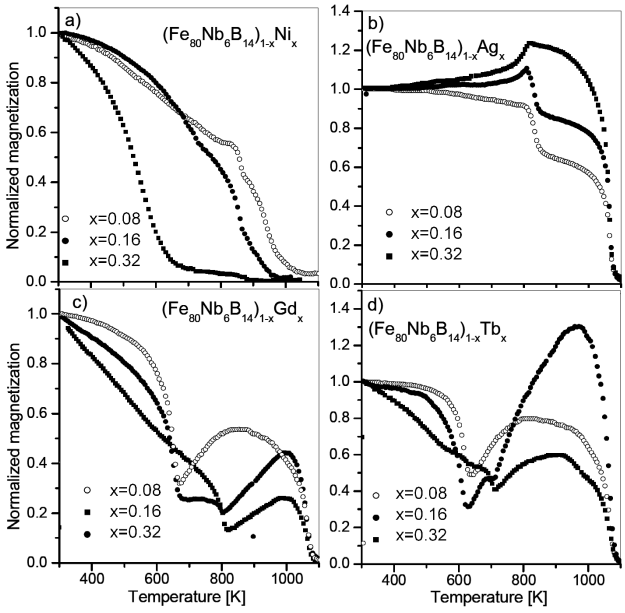

Fig. 3. Thermomagnetic curves $M(T)$ for all the studied alloys.

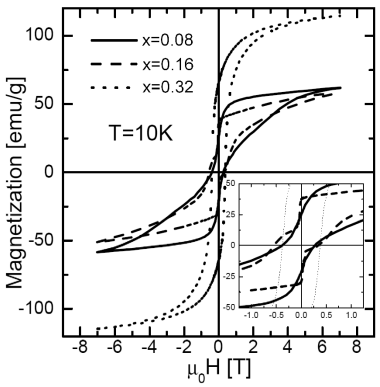

Fig. 4. Hysteresis loops for $(Fe_{80}Nb_6B_{14})_{1-x}Tb_x$ alloys measured at 10 K.

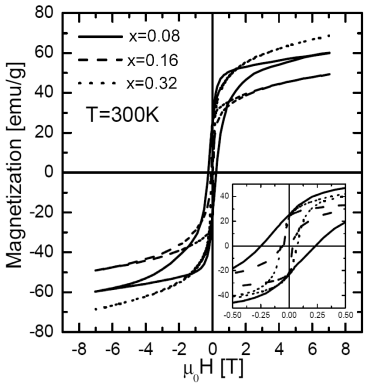

Fig. 5. Hysteresis loops for $(Fe_{80}Nb_6B_{14})_{1-x}Tb_x$ alloys measured at 300 K.

the $(Fe_{80}Nb_6B_{14})_{1-x}Tb_x$ alloy is depicted in Fig. 2. For all the studied cases the spectra were deconvoluted into a set of elementary Zeeman sextets by a least-squares fit procedure. One can see that the obtained spectra are complex and consist of many components that can be attributed to different binary and/or ternary compounds as well as to a paramagnetic Fe in nonmagnetic surroundings.

Table I summarizes the detected crystal phases, their mean grain diameters and an estimation of a percentage contribution. For 8 at.% of RE = Gd, Tb addition a formation of ternary $RE_2Fe_{14}B$ phases, as a main component, and binary one of $REFe_2$ were observed. For higher RE content the $REFe_2$ phase becomes dominant. Moreover, from the Mössbauer analysis an existence of about 10% of Fe in paramagnetic state (some iron separations inserted into non-magnetic matrix) for the tested cases is evident. The presented structural investigations confirms that the applied mould suction technique is favorable to nanocrystallization of the prepared bulk alloys. Figure 3 presents thermomagnetic curves $M(T)$ in the temperature range from 300 K to 1100 K for all the studied alloys. Such curves allow determining temperatures of magnetic transitions characteristic for different

crystal phases. The increase of magnetization observed with increasing temperature is surely related to crystallization of the residual amorphous phase. The latter was confirmed by a second run (not presented here) where the $M(T)$ increase was not observed.

Figures 4 and 5 present hysteresis loops measured at 10 K and 300 K for the $(Fe_{80}Nb_6B_{14})_{1-x}Tb_x$ alloys, respectively. Such low temperature measurements were carried out for all the studied alloys in the applied external magnetic field ±7 T. For the Tb rich sample ($x = 0.32$), according to the XRD and Mössbauer results, the shape of the loop is characteristic of homogeneous material (i.e. with one magnetic phase), while those of $x = 0.08$ and $x = 0.16$ the loops are characteristic for multi-magnetic structure.

All obtained results are listed in Table II. For the samples with M = Ag, Ni hysteresis loops were too small to determine their reliable parameters. However, for the $(Fe_{80}Nb_6B_{14})_{1-x}Ag_x$ alloys one can observe an increase of magnetic moment of Fe atoms from 2.26 μ_B to 3.36 μ_B for $x = 0.08$ and 0.32, respectively. The increase can be attributed to a formation of Fe–Ag clusters in which Fe atoms are more separated than in a pure iron. Such effect was observed in Fe/Ag thin multilayer systems [12] and is with agreement with theory predictions [13]. In the case of the $(Fe_{80}Nb_6B_{14})_{1-x}Ni_x$ alloys the decrease of μ_{MAG} can be explained by an increasing contribution of the Fe–Ni (fcc) phase. The magnetic hardening of the Gd and Tb doped alloys can be attributed to the formation of $RE_2Fe_{14}B$ phases, especially in the case of Tb due to its strong spin–orbit coupling. Taking into account the expected values of atomic magnetic moments and atomic compositions one can state that for $x = 0.08$ the Fe magnetic sublattice is dominant while for $x = 0.16$ and $x = 0.32$ the magnetization of RE site is higher. It seems that near a composition, for which these two magnetic sites are magnetically compensated, the influence of microstructure as well as crystal disorder on magnetic hardening is more efficient. Therefore, the $(Fe_{80}Nb_6B_{14})_{1-x}Tb_x$ bulk nanocrystalline alloy with the parameter x ranged from 0.08 to 0.16 should be very interesting from both scientific and practical point of view.

TABLE I

Crystal phases, percentage contribution of a given phase (* obtained from the Mössbauer spectra or XRD patterns) and mean diameter of the main phase D for the studied alloys.

Alloy	D [nm]	Phases	Contribution [%]
$(Fe_{80}Nb_6B_{14})_{0.92}Gd_{0.08}$	28	$Gd_2Fe_{14}B$, int. phase, $GdFe_2$ paramag.	77, 6, 5, 12
$(Fe_{80}Nb_6B_{14})_{0.84}Gd_{0.16}$	13	$Gd_2Fe_{14}B$, int. phase, $GdFe_2$, paramag.	59, 11, 17, 13
$(Fe_{80}Nb_6B_{14})_{0.68}Gd_{0.32}$	26	$GdFe_2$, Gd *	
$(Fe_{80}Nb_6B_{14})_{0.92}Tb_{0.08}$	28	$Tb_2Fe_{14}B$, $TbFe_2$, paramag.	80, 8, 12
$(Fe_{80}Nb_6B_{14})_{0.84}Tb_{0.16}$	16	$Tb_2Fe_{14}B$, $TbFe_2$, paramag.	59, 28, 13
$(Fe_{80}Nb_6B_{14})_{0.68}Tb_{0.32}$	25	$TbFe_2$, Tb_xFe_{2-x}, paramag.	83, 7, 10
$(Fe_{80}Nb_6B_{14})_{0.92}Ni_{0.08}$	12	Fe–Ni (bcc), Fe–B, paramag.	55, 34, 11
$(Fe_{80}Nb_6B_{14})_{0.84}Ni_{0.16}$	12	Fe–Ni (bcc/fcc), Fe–B, paramag.	52, 36, 12
$(Fe_{80}Nb_6B_{14})_{0.68}Ni_{0.32}$	14	Fe–Ni (fcc), Fe–B, paramag.	52, 42, 6
$(Fe_{80}Nb_6B_{14})_{0.92}Ag_{0.08}$	16	Fe (bcc), Fe–B, paramag.	42, 49, 9

TABLE II

Saturation magnetization M_S, magnetic moment per magnetic atoms μ_{MAG}, coercive field H_C, remanence to saturation ratio M_r/M_s, and energy product $|BH|_{max}$ for all the studied alloys.

Alloy	M_s (10 K) [emu/g]	μ_{MAG} [μ_B]	Alloy	M_s (10 K) [emu/g]	μ_{MAG} [μ_B]	H_c (10 K) [Oe]	H_c (300 K) [Oe]	M_r/M_s (10 K)	M_r/M_s (300 K)	$\|BH\|_{max}$ (10 K) [kJ/m^3]	$\|BH\|_{max}$ (300 K) [kJ/m^3]
$(Fe_{80}Nb_6B_{14})_{0.92}Ag_{0.08}$	158.6	2.26	$(Fe_{80}Nb_6B_{14})_{0.92}Gd_{0.08}$	79.5	1.08	660	680	0.23	0.25	2.50	2.7
$(Fe_{80}Nb_6B_{14})_{0.84}Ag_{0.16}$	165.0	2.91	$(Fe_{80}Nb_6B_{14})_{0.84}Gd_{0.16}$	77.2	1.20	700	1290	0.23	0.29	2.40	4.0
$(Fe_{80}Nb_6B_{14})_{0.68}Ag_{0.32}$	121.3	3.36	$(Fe_{80}Nb_6B_{14})_{0.68}Gd_{0.32}$	109.65	2.10	137	98	–	–	–	–
$(Fe_{80}Nb_6B_{14})_{0.92}Ni_{0.08}$	167.2	1.92	$(Fe_{80}Nb_6B_{14})_{0.92}Tb_{0.08}$	62.0	0.85	3890	2490	0.41	0.42	14.1	12.7
$(Fe_{80}Nb_6B_{14})_{0.84}Ni_{0.16}$	151.2	1.71	$(Fe_{80}Nb_6B_{14})_{0.84}Tb_{0.16}$	57.2	0.89	5460	540	0.65	0.46	23.9	2.8
$(Fe_{80}Nb_6B_{14})_{0.68}Ni_{0.32}$	137.7	1.53	$(Fe_{80}Nb_6B_{14})_{0.68}Tb_{0.32}$	114.6	2.21	3810	720	0.57	0.33	91.4	3.9

4. Conclusions

The main conclusions of the present paper, in relation to the $(Fe_{80}Nb_6B_{14})_{1-x}$ M_x (M = Ni, Ag, Gd, Tb and $x = 0.08$, 0.16, 0.32) alloys, can be summarized as follows:

(i) The applied mould suction technique is favorable in order to obtain nanocrystalline alloys. In our case the mean diameters of crystallites are ranged from about 10 nm to 30 nm. In the case of M = Gd, Tb the performed phase identification reveals a formation of ternary $RE_2Fe_{14}B$ and binary $REFe_2$ phases dependently on the alloy composition. (ii) For the alloys with M = Ag magnetic moment of Fe atom increases from 2.26 μ_B to 3.36 μ_B for $x = 0.08$ and $x = 0.32$, respectively. For M = Ni this quantity decreases with increasing x due to

appearing of Fe–Ni (fcc) phases. (iii) For M = Gd, Tb the alloys are ferrimagnetic with compensation composition ranged between $x = 0.08$ and $x = 0.16$. The both RE alloying additions cause a significant magnetic hardening especially in the case of Tb due to its strong spin–orbit coupling.

Acknowledgments

This work was supported by the Polish Ministry of Science and Higher Education under grant NN507 317336.

References

[1] M.E. McHenry, M.A. Willard, D.E. Laughlin, *Prog. Mater. Sci.* **44**, 291 (1999).

[2] G. Herzer, L.K. Varga, *J. Magn. Magn. Mater.* **215--216**, 506 (2000).

[3] H. Chiriac, N. Lupu, *J. Non-Cryst. Solids* **250-252**, 751 (1999).

[4] M. Stoica, S. Roth, J. Eckert, L. Schultz, M.D. Baro, *J. Magn. Magn. Mater.* **290-291**, 1480 (2005).

[5] K. Biswas, S. Ram, S. Roth, L. Schultz, J. Eckert, *J. Mater. Sci.* **41**, 3445 (2006).

[6] Q. Wang, C.L. Zhu, C. Dong, J.B. Qiang, W. Zhang, A. Inoue, *J. Phys. Conf. Ser.* **98**, 012017 (2008).

[7] A. Inoue, *Mater. Sci. Eng. A* **226-228**, 357 (1997).

[8] G. Haneczok, J.E. Frąckowiak, A. Chrobak, P. Kwapuliński, J. Rasek, *Phys. Status Solidi A* **202**, 2574 (2005).

[9] A. Chrobak, D. Chrobak, G. Haneczok, P. Kwapuliński, Z. Kwolek, M. Karolus, *Mater. Sci. Eng. A* **382**, 401 (2004).

[10] A. Chrobak, G. Haneczok, D. Chrobak, Ł. Madej, G. Chełkowska, M. Kulpa, *J. Magn. Magn. Mater.* **320**, e770 (2008).

[11] A. Chrobak, M. Karolus, G. Haneczok, *Solid. State Phenom.* **163**, 233 (2010).

[12] C.L. Wooten, J. Chen, G.A. Mulchollan, J.L. Erskine, J.T. Markert, *Phys. Rev. B* **49**, 10023 (1994).

[13] Y. Hashi, Zhi-Quang Li, K. Ohno, Y. Kawazoe, *Mater. Trans.* **37**, 279 (1996).